Available online at www.sciencedirect.com
ScienceDirect
Journal of Nuclear Materials 367–370 (2007) 858–863
journal of nuclear materials
www.elsevier.com/locate/jnucmat

Irradiation induced precipitates in vanadium alloys studied by atom probe microanalysis

N. Nita [a,*], Y. Anma [a], H. Matsui [a], T. Ohkubo [b], K. Hono [b]

[a] Institute for Materials Research, Tohoku University, Katahira 2-1-1, Aoba-ku, Sendai 980-8577, Japan
[b] National Institute for Materials Science, Tsukuba, Japan

Abstract

Radiation-induced titanium precipitates are a major cause of irradiation hardening in vanadium alloys, but microstructural information is still far from comprehensive. In particular, the nature of black dot clusters observed to form during irradiation at low temperatures is still not clear while the large size Ti-precipitates with platelet shapes are relatively well characterized. V–4Cr–(0.1, 1 and 3 wt%)Ti alloys were irradiated up to 0.2 dpa at 350 °C. In TEM observations, platelet precipitates on {1 0 0} planes were observed in V–4Cr–3Ti and V–4Cr–1Ti, while a high density of small defect clusters was observed as black dot contrast in V–4Cr–1Ti. Enrichment of titanium as well as oxygen and titanium oxide in the matrix were observed by three-dimensional atom probe microanalysis in all alloys. Small clusters with sphere shape were observed in V–4Cr–0.1Ti, while the platelet morphology was seen in the other alloys. The mechanisms of nucleation and growth of precipitates in vanadium alloys are discussed.

1. Introduction

Vanadium alloys are candidate materials for fusion reactors. Because of its good resistance to neutron irradiation, V–4Cr–4Ti, in particular, has been studied extensively in the past decades [1–3]. However, it has been reported that significant radiation hardening and embrittlement occurred in V–4Cr–4Ti irradiated by neutrons at relatively low temperatures [4,5]. For instance, Fukumoto et al. reported that neutron irradiation decreased uniform elongation by 40% and increased yield stress to 600 MPa [6]. In order to understand the mechanism of the hardening and embrittlement, microstructural observations using transmission electron microscope (TEM) have been conducted. According to previously reported TEM studies [7,8], radiation-induced titanium precipitates are the major cause of irradiation hardening, however the microstructural information is far from comprehensive. In particular, the nature of black dot clusters which were observed to form under irradiation at low temperatures is still not clear while the large size Ti-precipitates with platelet shapes are relatively well characterized. Higashiguchi et al. concluded that the detailed TEM investigation have clarified that these large precipitates are circular, planar coherent particles lying on {1 0 0} planes and have fcc structures [9], while Kazakov et al. reported that the precipitates are coherent or semi-coherent [10].

* Corresponding author. Tel.: +81 22 215 2068; fax: +81 22 215 2066.
E-mail address: nita@imr.edu (N. Nita).

0022-3115/$ - see front matter © 2007 Published by Elsevier B.V.
doi:10.1016/j.jnucmat.2007.03.069

The quantitative composition of these precipitates is not well understood, although many researchers have analyzed the diffraction patterns obtained from TEM and identified them as Ti_2O, Ti_5Si_3, Ti(OCN), $Ti_{16}(O_3C_2N_3)$, Ti(ON), etc [9–14]. The objective of this study was to investigate both the nature of black dot clusters formed under low temperature irradiation and the chemical composition of titanium rich precipitates in vanadium alloy. For the analysis of fine precipitates, three-dimensional atom probe microanalysis (3DAP) is a very powerful tool with its atomic scale spatial resolution. In the present paper, experimental results using 3DAP combined with TEM observation on fine Ti-precipitates in vanadium alloys are presented.

2. Experimental procedures

V–4Cr–(0.1, 1 and 3 wt%)Ti alloys were prepared. Table 1 shows the concentration of interstitial impurities in these alloys. The alloys were prepared by arc-melting in an argon atmosphere, followed by cold rolling to sheet of 0.25 mm thickness. TEM discs and dog bone shaped miniature tensile specimens were punched from the sheets and annealed at 1100 °C for 2 h in a high vacuum ($<2.0\times10^{-6}$ torr). Neutron irradiation was conducted in the Japan Material Testing Reactor (JMTR) up to 0.2 dpa at 350 °C. The damage rate was 9.4×10^{-8} dpa/s. After electro polishing, TEM observation was performed using a JOEL-2010 equipped with an energy dispersive X-ray spectrometry (EDX) detector. To prepare needle-like specimens for the 3DAP analysis, the irradiated tensile specimens were cut into small square rods of approximately $0.25\times0.25\times7$ mm, which were subsequently electropolished to blunt needles. Finally sharp needle tips were fabricated by focused ion beam (FIB) processing with an annular gallium ion beam of 30 keV. 3DAP measurements were carried out using energy compensated position-sensitive atom probe facilities which consists of a reflectron energy compensator, a position sensitive detector and a high-resolution flight time detector [15]. Measurements were conducted at a sample temperature of 60 K with pulse fraction 0.2 under ultra-high vacuum conditions.

Table 1
The concentration of interstitial impurities in vanadium alloys

	Oxygen (wppm)	Nitrogen (wppm)	Carbon (wppm)
V–4Cr–0.1Ti	693	40	76
V–4Cr–1Ti	735	37	62
V–4Cr–3Ti	545	73	34

3. Results

3.1. TEM observation

Fig. 1 shows the microstructures of V–4Cr–(0.1, 1 and 3)Ti alloys after neutron irradiation to 0.2 dpa at 350 °C. The beam directions were close to [001]. Line-shaped precipitates along ⟨100⟩ directions were observed in V–4Cr–1Ti and V–4Cr–3Ti. These precipitates were determined to be planar by tilting the samples under the microscope.

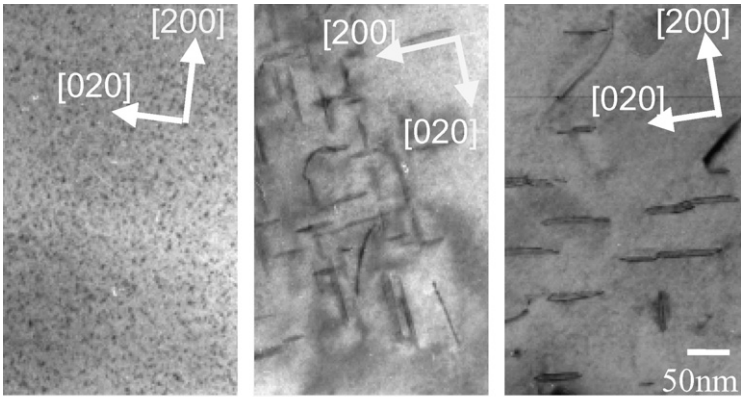

Fig. 1. The microstructures of V–4Cr–(0.1, 1 and 3)Ti after neutron irradiation to 0.2 dpa at 350 °C.

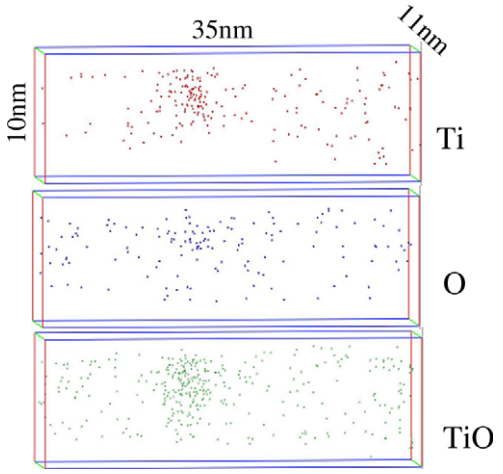

Fig. 2. The 3DAP elemental maps of Ti, O and TiO in V–4Cr–0.1Ti after neutron irradiation to 0.2 dpa at 350 °C.

Since precipitates were not observed in the unirradiated specimen, it is deemed that they were radiation induced precipitates and similar to the precipitates which have been reported in previous studies [4,8,12,16]. Comparing V–4Cr–1Ti and V–4Cr–3Ti, the average size of precipitates increased from 47 nm to 80 nm with increasing titanium concentration while the number density decreased from $1.1 \times 10^{21}\ m^{-3}$ to $7.1 \times 10^{20}\ m^{-3}$. Titanium was detected in these precipitates by elemental analysis using EDX while enrichment of other elements was not clearly detected. However, light elements such as oxygen, carbon and nitrogen are difficult to detect by an EDX technique.

A high density of black dot contrast centers was observed in V–4Cr–0.1Ti after neutron irradiation to 0.2 dpa at 350 °C. The number density and the average size of defect clusters were $4.6 \times 10^{22}\ m^{-3}$ and 4.1 nm, respectively. It was difficult to determine whether these fine defect clusters were precipitates or dislocation loops because they did not show the contrasts of planar shapes and titanium was not clearly detected by EDX analysis due to their small sizes.

3.2. Three-dimensional atom probe analysis

Fig. 2 shows the 3DAP elemental maps of Ti, O and TiO in V–4Cr–0.1Ti after neutron irradiation to 0.2 dpa at 350 °C. Enrichment of titanium, oxygen and titanium oxide in the matrix were observed, although EDX measurements could not detect titanium in the fine defect clusters due to their small sizes. These fine clusters may correspond to the black dot defect clusters observed by TEM. This defect cluster was spherical with diameter about 1.5 nm. It should be noted that the interface between the defect cluster and the matrix was not well defined and there was no enrichment of carbon, nitrogen or other elements at the defect cluster.

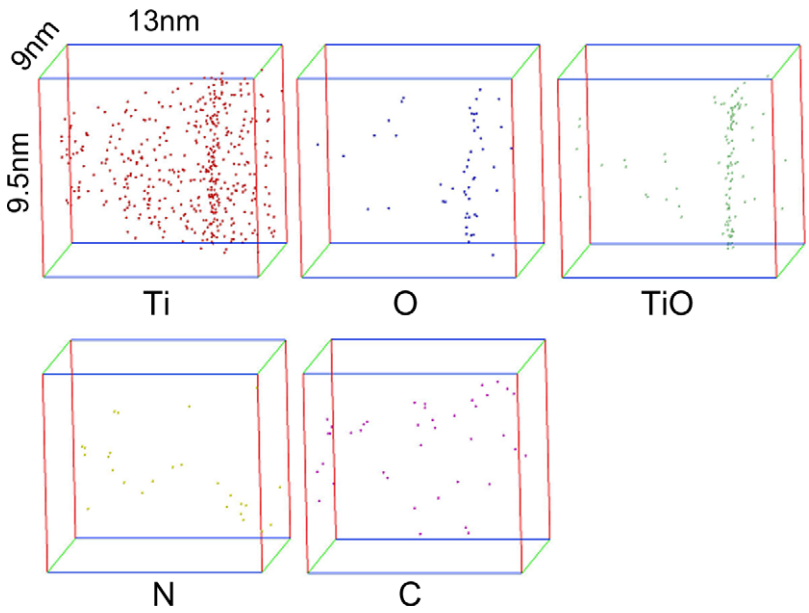

Fig. 3. The 3DAP elemental maps of Ti, O, TiO, N and C in V–4Cr–1Ti after neutron irradiation to 0.2 dpa at 350 °C.

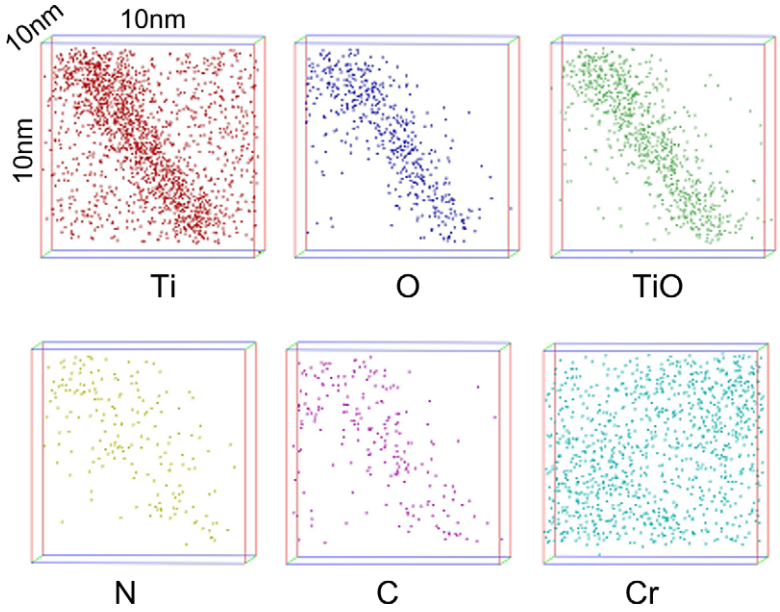

Fig. 4. The 3DAP elemental maps of Ti, O, TiO, N, C and Cr in V–4Cr–3Ti after neutron irradiation to 0.2 dpa at 350 °C.

Fig. 3 shows the 3DAP elemental maps of Ti, O, TiO, N and C in V–4Cr–1Ti after neutron irradiation to 0.2 dpa at 350 °C. A high local concentration of titanium, oxygen and titanium oxide was observed, with no change in concentration of nitrogen and carbon. This corresponds to the precipitates observed by TEM. The orientation of this precipitate was viewed edge on and its morphology was identified as a platelet by viewing these elemental maps from another directions. The thickness of this platelet shaped precipitate was 1.2 nm and the length perpendicular to the habit plane of the precipitate was longer than the 9.5 nm of analyzed volume.

Fig. 4 shows the 3DAP elemental maps of Ti, O, TiO, N, C and Cr in V–4Cr–3Ti after neutron irradiation to 0.2 dpa at 350 °C. A platelet shaped precipitate was observed edge on. Not only titanium, oxygen and titanium oxide but also nitrogen and carbon were enriched in the precipitate in this alloy. On the other hand, chromium was slightly depleted at the precipitate. The thickness of the platelet was 2 nm and the size perpendicular to the platelet was extended beyond the analyzed volume. The precipitate was thicker in the V–4Cr–3Ti alloy than in the V–4Cr–1Ti. This is good agreement with the results of TEM observation, although the volumes analyzed by 3DAP were too small to compare the whole precipitates.

4. Discussion

4.1. Nucleation mechanism for precipitates in vanadium alloys

A high density of black dot contrast defects was observed in V–4Cr–0.1Ti. Similar black dot contrast has often been reported in vanadium alloys irradiated at low temperature [4,5,7] and it was difficult to determine the nature of these fine defect clusters by conventional TEM equipped with EDX analysis. In the present work, spherical zones enriched in titanium and oxygen were observed by 3DAP. It is surmised that the cluster observed by 3DAP corresponds to the black dot contrast features observed by TEM, although the size of cluster detected by 3DAP was about 3 nm while the size of the black dot was about 1 nm when viewed by TEM. This difference in size could be because the interface between the small cluster and the matrix was poorly defined, compared to the larger precipitates detected in V–4Cr–1Ti and V–4Cr–3Ti. This indicates that the defect cluster does not have a specific structure like a compact precipitate. The morphology of the cluster is more like an atmosphere or enriched zone of titanium and oxygen. It was deduced that titanium and oxygen segregated to dislocation loops and formed atmospheres there.

Table 2
The chemical compositions, ratio of oxygen to titanium and the shape of defect clusters derived from atom probe selected area analyses

	Composition (at.%)	O/Ti ratio	Shape
V–4Cr–0.1Ti	$Ti_{5.67}O_{5.23}N_{0.04}C_{0.04}V_{70}Cr_{3.75}$	0.92	Sphere
V–4Cr–1Ti	$Ti_{7.47}O_{4.09}N_{0.05}C_{0.08}V_{65}Cr_{3.2}$	0.54	Platelet
V–4Cr–3Ti	$Ti_{40}O_{25.3}N_{4.8}C_{5.1}V_{39}Cr_1$	0.63	Platelet

Namely, defect clusters observed by TEM were dislocation loops while the atmosphere was observed by 3DAP.

Moreover, it could be also deduced that the observed spherical cluster are the nucleation stage of precipitates. In other words, the nucleation of titanium-rich precipitates might start with the segregation of titanium and oxygen to dislocation loops.

4.2. Growth mechanism of precipitates in vanadium alloys

Detailed analyses by 3DAP were adopted to understand the growth mechanism of precipitates in vanadium alloys. Table 2 shows the chemical compositions, ratio of oxygen to titanium and the shape of defect clusters derived from atom probe selected area analyses. Larger defect clusters were observed with increasing concentration of titanium in vanadium alloys. Nitrogen and carbon were also contained in the large platelet shape precipitates in V–4Cr–3Ti while no nitrogen or carbon enrichment was observed with smaller precipitates, although the impurity levels were comparable and these impurities had enough mobility at irradiation temperature of 350 °C [17,18]. This will be explained by the difference in the extent of strain fields. Lager precipitates should have a larger strain field because these precipitates are coherent or semi-coherent. Small clusters were spherical and their elemental ratio of oxygen to titanium was 0.92 while larger clusters were planar and the ratios were 0.54 and 0.63. It is likely that the precipitates grow by changing their morphology from sphere to platelet and changing the ratio of titanium to oxygen. In other words, the spherical cluster during the nucleation stage is TiO and the planar cluster during the growth stage is Ti_3O_2. Since precipitates in vanadium alloys were determined to have fcc structure of the NaCl type, it could be pointed out that the planar precipitates contain vacancies. Carbon and nitrogen will be absorbed easily at the sub-lattice sites of oxygen during the growth stage.

5. Conclusion

Neutron irradiated vanadium alloys were examined by TEM and 3DAP. A high density of small defect clusters was observed as black dot contrast in V–4Cr–1Ti. Although it was difficult to determine the nature of these fine defect clusters by conventional TEM using EDX technique, enrichment of titanium as well as oxygen and titanium oxide in the matrix were observed by 3DAP microanalysis. It is deduced that the spherical cluster was in the nucleation stage of precipitate formation. That is, the nucleation of titanium-rich precipitates might start with the segregation of titanium and oxygen to dislocation loops. It is also believed that the precipitates grow by changing their morphology from sphere to platelet and by changing the ratio of titanium to oxygen. The spherical cluster during the nucleation stage is TiO and the planar cluster during the growth stage is Ti_3O_2.

Acknowledgements

The authors are grateful to Dr M. Narui and the member of JMTR for neutron irradiation. The authors would like to thank T. Toyama for his technical assistance and valuable discussion. This work was partly supported by NIFS Budget Code NIFS05KFRF018.

References

[1] H. Matsui, K. Fukumoto, D.L. Smith, H.M. Chung, W.V. Witzenburg, S.N. Votinov, J. Nucl. Mater. 233–237 (1996) 92.
[2] H.M. Chung, B.A. Loomis, D.L. Smith, J. Nucl. Mater. 239 (1996) 139.
[3] B.A. Loomis, D.L. Smith, J. Nucl. Mater. 191–194 (1992) 84.
[4] N. Nita, K. Fukumoto, A. Kimura, H. Matsui, J. Nucl. Mater. 271&272 (1999) 365.
[5] E.V. van Osch, M.I. de Vries, J. Nucl. Mater. 271&272 (1999) 162.
[6] K. Fukumoto, H. Matsui, H. Tsai, D.L. Smith, J. Nucl. Mater. 283–287 (2000) 492.
[7] Y. Candra, K. Fukumoto, A. Kimura, H. Matsui, J. Nucl. Mater. 271&272 (1999) 301.

[8] N. Nita, T. Iwai, K. Fukumoto, H. Matsui, J. Nucl. Mater. 283–287 (2000) 291.
[9] Y. Higashuiguchi, H. Kayano, S. Morozumi, J. Nucl. Mater. 133&134 (1985) 662.
[10] V.A. Kazakov, Z. Ostrovsky, Yu. Goncharenko and V. Chakin 283–287 (2000) 727–730.
[11] D.S. Gelles, P.M. Rice, S.J. Zinkle, H.H. Chung, J. Nucl. Mater. 258–263 (1998) 1380.
[12] K. Fukumoto, H. Matsui, Y. Candra, K. Takahashi, H. Sasanuma, S. Nagata, K. Takahiro, J. Nucl. Mater. 283–287 (2000) 535.
[13] K. Fukumoto, H.M. Chung, J. Gazda, D.L. Smith, H. Matsui, Sci. Rep. RITU A 45 (1997) 149.
[14] S.J. Zinkle, N. Hashimoto, D.T. Hoelzer, A.L. Qualls, T. Muroga, B.N. Singh, J. Nucl. Mater. 307–311 (2002) 192.
[15] K. Hono, Prog. Mater. Sci. 47 (2002) 621.
[16] N. Nita, T. Yamamoto, T. Iwai, K. Yasunaga, K. Fukumoto, H. Matsui, J. Nucl. Mater. 307–311 (2002) 398.
[17] J.T. Stanley, Acta Metall. 20 (1972) 191.
[18] T. Shikama, J. Nucl. Mater. 68 (1977) 315.